Journal Pre-proof

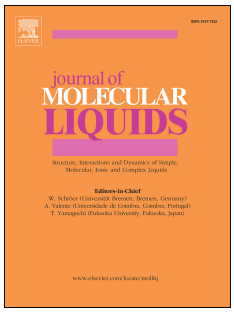

Development of nematic and orthogonal smectic phases in short-core fluorinated hockey-stick shaped liquid crystal compounds

Kalpana Upadhyaya, Sharmistha Ghosh, Raj Kumar Khan, R. Pratibha, Nandiraju V.S. Rao

PII: S0167-7322(17)35002-X

DOI: https://doi.org/10.1016/j.molliq.2019.111989

Reference: MOLLIQ 111989

To appear in: *Journal of Molecular Liquids*

Received Date: 20 October 2017

Revised Date: 29 July 2019

Accepted Date: 20 October 2019

Please cite this article as: K. Upadhyaya, S. Ghosh, R.K. Khan, R. Pratibha, N.V.S. Rao, Development of nematic and orthogonal smectic phases in short-core fluorinated hockey-stick shaped liquid crystal compounds, *Journal of Molecular Liquids* (2019), doi: https://doi.org/10.1016/j.molliq.2019.111989.

Development of nematic and orthogonal smectic phases in short-core fluorinated hockey-stick shaped liquid crystal compounds

Kalpana Upadhyaya[a], Sharmistha Ghosh*[b], Raj Kumar Khan [b], R. Pratibha[c] and Nandiraju V. S. Rao*[a]

[a]Chemistry Department, Assam University, Silchar 788011, India,
[b]Department of Physics, University of Calcutta, 92 A PC Road, Kolkata 700 009, India,
[c]Raman Research Institute, C. V. Raman Avenue, Sadashivanagar, Bangalore 560 080, India

Abstract:

Here we report synthesis and investigations on novel short-core hockey-stick shaped molecules bearing a 4-n-alkyloxy-2-hydroxybenzylidene moiety at one end and polar fluoro-biphenyl moiety at the other end. The polar chloro and fluoro substituent at the lateral position of the core confers nematic and orthogonal smectic mesomorphism. The mesophase morphology is characterized by polarizing optical microscopy (POM), differential scanning calorimetry (DSC), X-ray diffraction (XRD), electro-optical study and dielectric spectroscopy. The fluorinated compounds **1b** (n=16) **and 1c** (n=18) have long terminal hydrocarbon tail and show orthogonal smectic phases with antiferroelectric switching behavior. The chlorinated compound **2e** (n=8) with relatively short terminal chain length exhibits only a monotropic nematic phase on cooling. The nematic phase is comprised of cybotactic clusters as confirmed by XRD and exhibits electro-optic switching. The compound **2i** (n=12) manifests a short range enantiotropic nematic and additional orthogonal smectic phase. Dielectric spectroscopy reveals polar correlations in the nematic and smectic phases.

1. Introduction:

Dipolar intermolecular interactions stabilize the macroscopic polarization density, characteristic of ferroelectric phases, in crystals. When the crystal is transformed into anisotropic layered fluid the dipolar interactions become weak and hence the realization of ferroelectricity is dependent on parallel alignment of the molecular dipoles within each layer. The most attractive features of achiral bent-core compounds[1-4] are their unusual mesomorphic behaviour, polar order,[5-10] and macroscopic chirality[11]. Recently ferroelectric properties have been unambiguously demonstrated in the orthogonal fluid smectic ($SmAP_F$ and $SmAP_{Fmod}$) phases exhibited by bent-core molecules possessing carbosilane moiety at one end and polar cyano or trifluoromethyl moieties at other end of the molecule as terminal substituents.[1-10] Further orthogonal polar smectic phase with alternating polar order in adjacent layers ($SmAP_A$) is reported in compounds of unsymmetrical achiral banana shaped molecules.[12-18] Very recently, achiral unsymmetrical bent-shaped molecules possessing a layered, optically uniaxial, orthogonal polar ordered structure with random direction of the layer polarization exhibiting

$SmAP_R$ phase[19-24] (SmA- stands for orthogonal smectic phase, P for polar layers and subscript R stands for random orientation of polarization in adjacent layers) is reported in few compounds. The polar orthogonal smectic phases are found to possess excellent potential applications to develop fast electro-optic devices. However an orthogonal smectic phase with overall polar order[9-24] is rare and is an experimental challenge which needs special molecular design.

Bent-core nematic (BCN) phase has been potentially attractive from both scientific understanding and application perspective owing to remarkable features like biaxiality[25], ferronematic phase[26-29], giant flexoelectricity (which is yet to be confirmed)[30] and twist-bend nematic phase[31-33]. Polar dynamics of electro-optic switching in biaxial bent-core nematic liquid crystal was first observed by Lee et.al, in an 1,3,4-oxadiazole based bent core LC[27(a)]. However the interpretation of the current peaks was based on biaxiality of the system which was not proved unambiguously and also was not in line with the symmetry arguments of LC[27(b)]. Later similar bent-core molecules based on 1,2,4-oxadiazole core were reported exhibiting ferroelectric switching in the nematic phase and the effect was attributed to reorganization of the polar cybotactic groups.[28-29] The existence of the cybotactic clusters was proved explicitly on the basis of X-ray diffraction, computer simulation, dielectric measurements etc. Dielectric spectroscopy in the cybotactic nematic phase revealed a peak with very large dielectric strength appearing at low frequency region corresponding to relaxation of cybotactic clusters. However achieving stable BCN was difficult as most of the BC molecules prefer stacking into layers owing to steric interaction and form banana phases. To prohibit the tendency of the bent-core molecules to lock into layers and promote stable nematic phases several tailoring in the molecular structure were required such as substitution of bulky moiety at the core or asymmetry in the terminal chains etc.[34] Another promising approach was to reduce the number of benzene rings in the core or/and reduce the bend angle. Wide range of nematic phases has been successfully developed in four ring bent-core LCs with reduced bend angle (~145°).[35-37] Further, ferroelectric-like switching in the nematic phase in a four-ring compound has been reported recently[35].

Molecular architecture at the interface of conventional rod-like and bent-core molecules is utmost important owing to their distinct structure-property relationship. One such structure is hockey-stick shaped molecule where one arm of a bent-core is significantly larger than the other. These molecules have attracted growing attention since they help us understand how self-assembly of asymmetric molecules leads to development of varieties of mesophases[38-41].

Here we report two homologous series of hockey-stick liquid crystals with the same core structure but having either chloro- or fluoro- lateral substituents at one of its rings. The

molecular architecture is such that there is reduction in rotational disorder as well as a strong dipole lies in the bent direction, facilitating orthogonal polar phases. The mesophase morphology is characterized by polarizing optical microscopy (POM), differential scanning calorimetry (DSC), X-ray diffraction (XRD), electro-optical and dielectric spectroscopy. It is found that the chlorinated compound with short terminal chain length **2e** (n=8) exhibits only a monotropic nematic phase on cooling. The nematic phase is comprised of cybotactic clusters as confirmed by XRD and dielectric spectroscopy. The higher homologue **2i** (n=12) manifests a short range enantiotropic nematic and an additional orthogonal smectic phase whereas the other two compounds **1b** (n=16) **and 1c** (n=18) show only polar orthogonal smectic phases with antiferroelectric switching behavior. Dielectric spectroscopy reveals polar correlations in the nematic and smectic phases.

2. Experimental:

2.1 General methods:

We have synthesized two homologous series **1a-1c** and **2a-2i**. Among the **1a-1c** homologous series the n-heptyloxy homologue did not exhibit liquid crystalline phase while the n-octadecyloxy exhibited monotropic phase. The n-hexadecyloxy homologue, **1b,** exhibited enantiotropic orthogonal smectic A phase with polar characteristics and will be described in the next section. In the **2a-2i** homologous series the lower homologues of n-butyloxy to n-octyloxy homologues exhibited monotropic nematic phase, while the n-nonyloxy to n-undecyloxy homologues exhibited monotropic nematic and orthogonal smectic A phases. However the n-dodecyloxy homologue **2i** exhibited enantiotropic nematic and smectic A phases. In this manuscript we have presented the results on four hockey-stick shaped samples viz., **1b** and **1c** of the homologous series I and **2e** and **2i** of the series II. Both homologous series possess essentially the same core except the lateral fluorine atom in series I is substituted by chlorine atom in series II. The samples were filled in planar aligned cells (E.H.C Japan), at temperatures well above their isotropic transition temperatures. The cell is consisted of two parallel glass plates whose inner surfaces are first coated with ITO and then a homogeneous aligning material (Polyvinyl alcohol). Finally the two plates are rubbed in antiparallel directions and mylar spacers are used to maintain uniform thickness of the cell. Dielectric measurements are done in 10µm thick cells whereas 4µm cells are used to study the electro-optical properties of the samples. The temperature of the cells was controlled by a Mettler FP82 hot stage attached to a FP90 temperature controller. For electro-optic measurement, HP33120A signal generator, F10A voltage amplifier and DL1620 oscilloscope were used. Current response was studied by polarization reversal method using a triangular wave field. Dielectric data were recorded in the

frequency range from 10Hz to 13MHz using a HP4192A Impedance Analyzer. Thermal behaviour of the samples was studied using differential scanning calorimetry (DSC) and texture was observed by polarizing microscope (DMLP, Leica).X-ray diffraction studies were carried on the compound **2e** on powder samples using CuKα radiation and the DY 1042-Empyrean Diffractometer System.

2.2 Design and General Synthetic procedures of the hockey-stick compounds:

The hockey-stick liquid crystals bearing a 4-n-alkyloxy-2-hydroxybenzylidene moiety at one end and the replacement of an azobenzene or 2-hydroxybenzylidene or phenyl benzoate unit in the longer arm of the bent molecule by a polar fluoro-biphenyl moiety, which lends stiffness to the molecule with a strong dipole moment in the lateral direction, were designed. Further the introduction of a 2-chloro moiety or 2,6-difluoro substituents in the 1,3-disubstituted phenyl ring of a hockey-stick molecular architecture can generate an obtuse bend angle of ~145°, which gives rise to an increase in bend angle as well as a strong dipole in the bending direction. The reduced bend from ~120 to ~145° of the 1,3-phenyl moiety by the introduction of a chloro moiety in the 2-position or fluoro substituents in 2- and 6- positions and with the decrease in the number of rings from five or more to four in the molecular unit, places these compounds at the borderline between classical rod-like LCs and bent-core mesogens. A combination of the lateral dipole in the form of a fluoro-biphenyl moiety in one of the arms of the bent-core molecule, while the central bent core possesses a chloro moiety projected at a location inside the molecular core to represent the transverse dipole or the projected 2-, 6- difluoro substituents contribute towards the transverse (2-fluoro) dipole as well as lateral (6-fluoro) dipole. The other end of the molecule is linked to 4-*n*-alkyloxy-2-hydroxybenzaldehyde through an imine moiety, which actually seems superior to the benzylidene aniline core and is more stable towards hydrolysis due to intramolecular hydrogen bonding. The realization of such a molecular architecture leads to a reduction in rotational disorder as well as a strong dipole in the bent direction. If molecular interactions are strong enough then the molecular structure can promote polar biaxial nematic or smectic phases.

The starting material in the present study 4-n-alkyloxy-2-hydroxybenzaldehyde was prepared by Williamson etherification of 2, 4-dihydroxybenzaldehyde with appropriate n-alkyl bromide. 2-chloro-3-nitrobenzoicacid and 2-, 6-difluoro-3-nitrobenzoicacid were converted into corresponding amines by reduction under balloon pressure filled with hydrogen gas using 5%

Pd-C. The crude products were then purified by column chromatography (silica gel 60-120 mesh, using dichloromethane/ethanol, (99.5:0.5::V/V) as eluent to give pure products 3-amino-2-chlorobenzoicacid and 2-, 6-difluoro-3-aminobenzoicacidrespectively. 3-amino-2-chlorobenzoicacid was condensed with 4-n-octyloxy (or n-dodecyloxy)-2-hydroxybenzaldhyde in presence of few drops of glacial acetic acid to get 3-[N-(4-n-octyloxy (or n-dodecyloxy) 2-hydroxybenzylidene)] amino 2-cholorobenzoicacid in good yields. 2-, 6-difluoro-3-aminobenzoicacidwas condensed with 4-n-hexadecyloxy (or n-octadecyloxy)-2-hydroxybenzaldhyde in presence of few drops of glacial acetic acid to get 4-[N-(4-n-hexadecyloxy (or n-octadecyloxy) 2-hydroxybenzylidene)amino]-2,6-difluorobenzoicacid in good yields. 3-[N-(4-n-octyloxy (or n-dodecyloxy) 2-hydroxybenzylidene)]amino 2-cholorobenzoicacid was further esterified with 4'-fluoro-[1,1'-biphenyl]-4-ol using DCC-DMAP reaction to yield the designed products **2e** and **2i.** 4-[N-(4-n-hexadecyloxy (or n-octadecyloxy) 2-hydroxybenzylidene) amino]-2,6-difluorobenzoicacid was further esterified with 4'-fluoro-[1,1'-biphenyl]-4-ol using DCC-DMAP reaction to yield the designed products **1b** and **1c** (Scheme 1)**.** The compounds were further recrystallized repeatedly from ethanol to get the pure samples. Elemental analyses of all the compounds were consistent with the proposed molecular formulae. All the compounds were characterized by FTIR, UV-Vis and ^{1}H NMR studies. The synthetic procedures for all the proposed compounds as detailed in **scheme 1** and characterization of the compounds **1a-1c and 2a-2i** (Scheme 1) by elemental analysis and spectroscopic data are described in electronic supporting information (ESI). The assigned $\nu_{O\text{-}H—N}$ stretching band confirmed the presence of intermolecular H-bonding in all the compounds. The introduction of ortho hydroxyl group in benzylidene moiety not only enhances the stability of the imines through intramolecular H-bonding to overcome the hydrolytic instability of the molecules towards moisture but also enhances the transverse dipole-moment. The infrared spectra of all the compounds exhibited characteristic bands in region 1625~1631 cm^{-1} ($\nu_{CH=N}$, imine), 1743~1755 cm^{-1} ($\nu_{C=O}$, ester), 3045~3201 cm^{-1} ($\nu_{O\text{-}H}$, H-bonding).

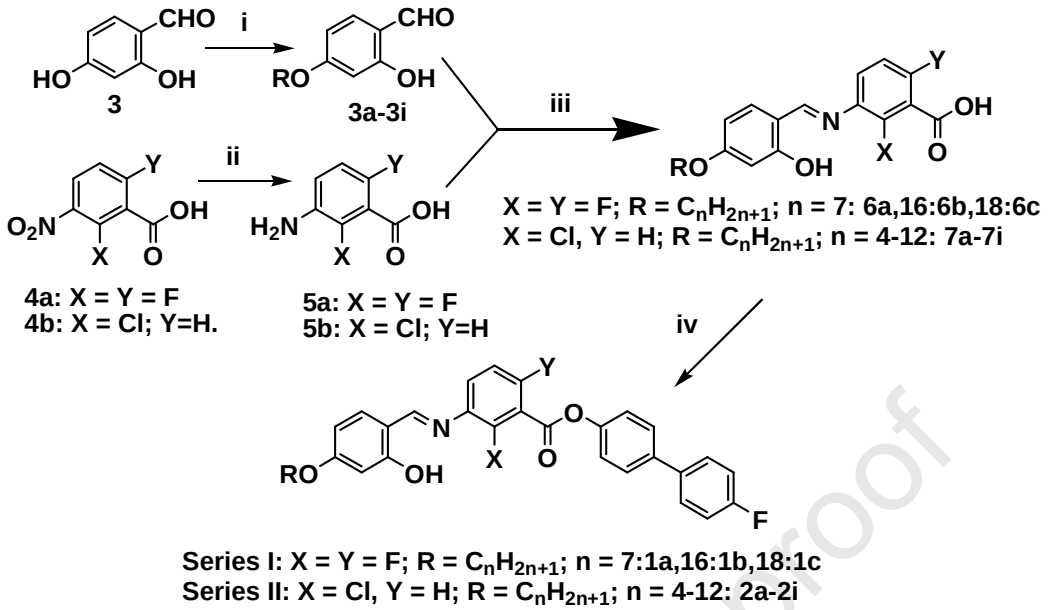

Scheme 1: Synthetic details of compounds **1a - 1c, 2a- 2i**. Reagent and conditions: i. Dry acetone $KHCO_3$, $C_nH_{2n+1}Br$ (*n* = 4-12, 16, 18); KI, Δ, 48 h; ii. 5% Pd/C, H_2, EtOAc stirring 24 h; iii. Abs EtOH, AcOH, Δ, 6 h; iv. DCC, DMAP, DCM, stirring 48 h.

TABLE 1: Phase transition temperatures (°C) and liquid crystalline phase thermal range of the compounds **1a-1c (n = 7, 16, 18)** and **2a-2i (n = 4- 12)** recorded for second heating (first row) and second cooling (second row) cycles at 5°C/min from DSC and confirmed by polarized optical microscopy. The enthalpies (ΔH in kJ/mol) and entropies (ΔS in J/mol.K) respectively are presented in parentheses.

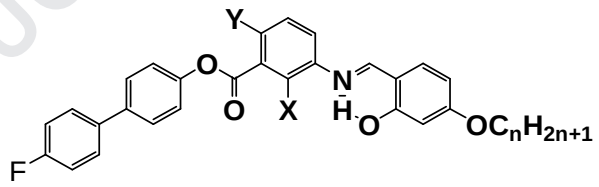

Code	n	X	Y	Phase transition temperatures °C (enthalpy kJ/mol; entropy J/mol.K))
1a	7	F	F	Cr 114.2 (28.3, 73.2) Iso Cr 126.4 (28.3, 70.9) Iso
1b	16	F	F	Cr 114.8(22.6, 58.4) SmA 117.9(9.75, 24.9) Iso Cr 101.2 (27.4, 73.4) SmA 116.1(8.15, 20.9)Iso
1c	18	F	F	Cr 117.8 (61.9, 158.4) Iso

				Cr 99.0 (54.9, 147.6) SmA 112.6 (11.2, 29.0) Iso
2a	4	Cl	H	Cr 122.9 (35.9, 90.9) Iso Cr 83.5 (20.7, 58.2) N 110.7 (0.085, 0.22) Iso
2b	5	Cl	H	Cr 117.2 (26.7, 68.6) Iso Cr 74.2 (14.3, 41.3) N 106.4 (0.13, 0.35) Iso
2c	6	Cl	H	Cr 133.2 (28.0, 68.9) Iso Cr 79.0 (9.80, 27.8) N 105.4 (0.15, 0.41) Iso
2d	7	Cl	H	Cr 114.5 (34.7, 89.7) Iso Cr 92.9 (30.2, 82.6) N 100.5 (0.15, 0. 41) Iso
2e	8	Cl	H	Cr 112.3 (32.6, 84.6) Iso Cr 88.8 (26.6, 73.7) N 103.7 (0.15, 0.40) Iso
2f	9	Cl	H	Cr 112.3 (34.8, 90.5) Iso Cr 78.0 (24.5, 70.0) SmA 85.3 (0.22, 0. 63) N 103.1 (0.18, 0.48) Iso
2g	10	Cl	H	Cr 109.0 (27.9, 72.9) Iso Cr 85.0 (20.9, 58.6) SmA 96.9 (0.33, 0.89) N 106.1 (0.23, 0.62) Iso
2h	11	Cl	H	Cr 104.8 (38.3, 101.4) Iso Cr 76.3 (31.3, 89.7) SmA 101.8 (0.88, 2.35) N 105.0 (0.30, 0.79) Iso
2i	12	Cl	H	Cr 106.2 (27.0, 71.2) SmA 108.9 (0.83, 2.18) N 109.5 (0.45, 1.18) Iso Cr 78.0 (24.1, 68.7) SmA 108.4 (1.27, 3.33) N 109.0 (0.47, 1.24) Iso

3. Results and discussions:

3.1 DSC and Polarizing optical microscopy:

The phase transition temperatures are determined through differential scanning calorimetry (DSC) at a scan rate of 5°C in both heating and cooling cycles (Supplementary). A representative DSC plot for the compound **2i** is shown in **Figure 1**.

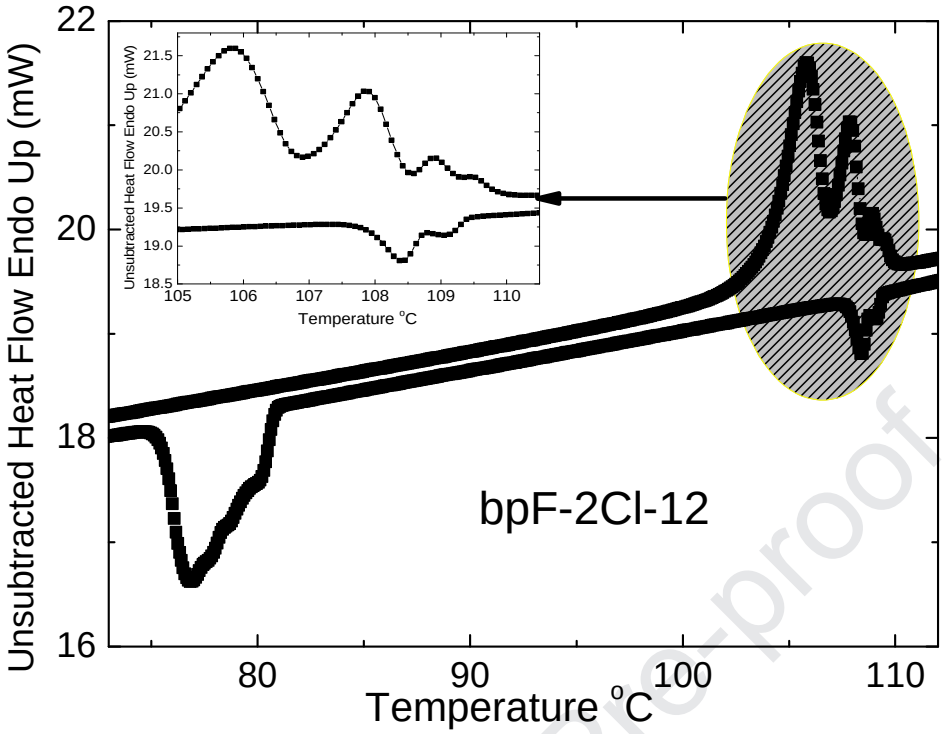

*Figure 1. DSC plot of the compound **2i** at a scan rate of 5°C in both heating and cooling cycles.*

The phase transitions of these compounds are further confirmed by polarizing optical microscopy (POM) and summarized in **Table 1**. The compounds **1b** and **1c** exhibit fan shaped textures typical for smectic A phase in non-treated cell on cooling (**figure 2(a)** and **2(d)**). In planar cells before and after applying electric field, the extinction regions are parallel to the direction of polarizer and analyzer (**figure 2(b)** and **2(e)**). After the a.c. electric field is applied, electro-optical switching along with textural changes occurred with a simultaneous change in birefringence (**figure 2(c)** and **2(f)**). The increase in birefringence is attributed to rotation of the local polar domains towards the electric field direction. The lower homologue **1a** of this series was not mesogenic (table 1).

Substitution of fluorine atom in the transverse direction by another electronegative atom chlorine and the lateral fluorine by hydrogen dramatically changes the character of the formed mesogens. **2e** shows a nematic phase on cooling. It exhibits characteristic marble textures in cells without any aligning layer (**figure 2(g)**), while homogeneous alignment was observed in planar cell (**figure 2(h)**). Under electric field, the change of birefringence is clearly observed (**figure 2(i)**). The optical response varies quadratically with applied electric field and indicates dielectric reorientation of the molecules. Another higher homologue of this series **2i** shows polymorphism, i.e. an additional nematic to SmA phase transition although the nematic range is

very small (~0.5^{O}C). The SmA phase has striped pattern in planar cells which turns to nematic-like texture after application of electric field (20V/µm) suggesting that the width of the stripes are reduced considerably (**figure 2(k)-(l)**). These changes of textures upon application of electric field phases indicate that the molecules are actually reorienting and the phase cannot be paraelectric in nature. The current response is confirmed further the polar properties of these phases.

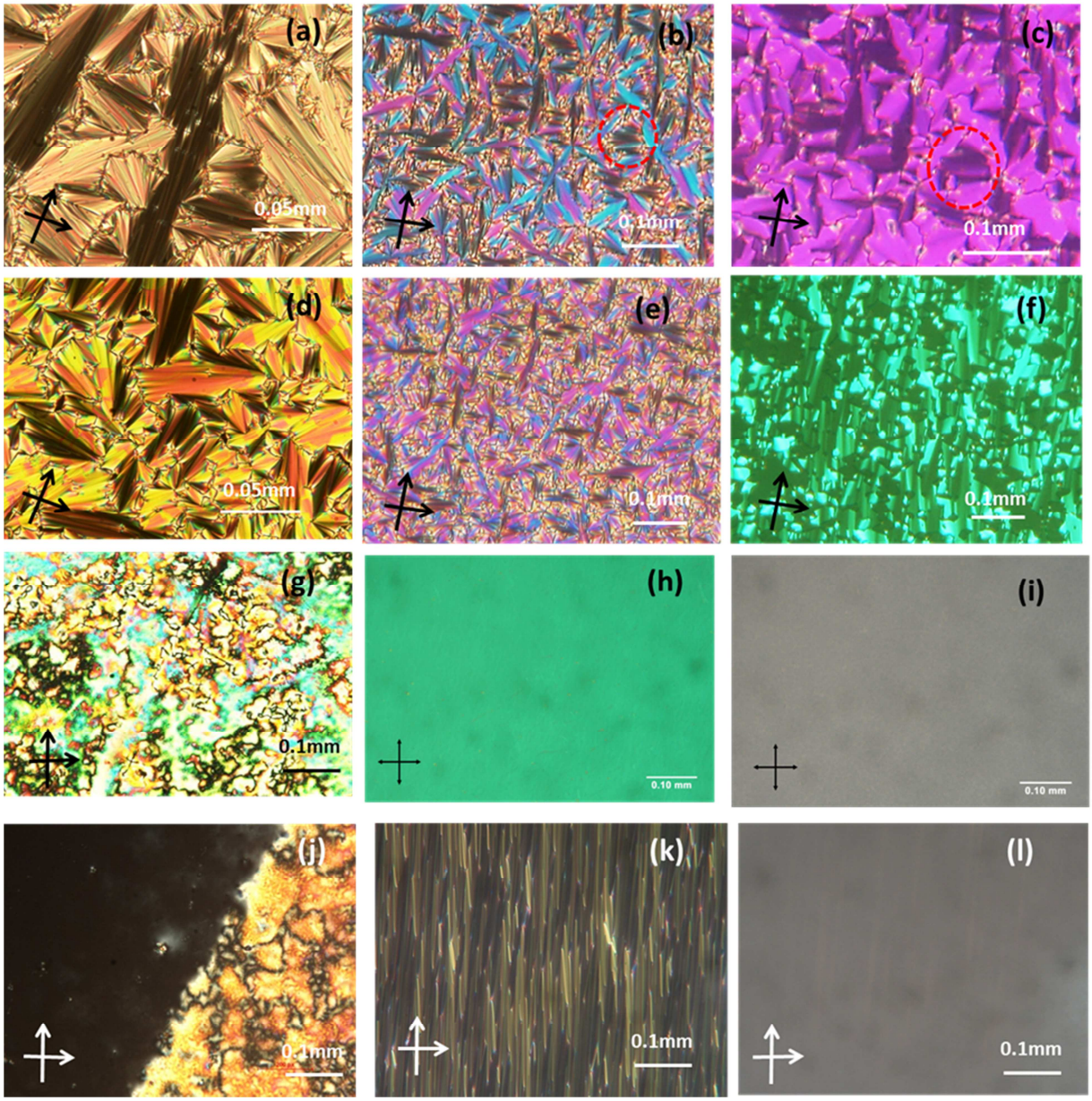

Figure 2. Optical micrographs during cooling for (a) ***1b*** *at 108°C (SmA phase) in non-treated glass plates, (b)* ***1-b*** *at 108°C in 10µm planar cell & (c)* ***1b*** *at 108°C in 10µm planar cell*

applying electric field 15V/µm, 10Hz ; (d) ***1c*** *at 104°C (SmA phase) in nonaligned glass plates, (e)& (f)* ***1c*** *at 105°C with applied electric field 0V and 15V/µm, 10Hz, (g)* ***2e*** *at 98°C in N phase in non-treated glass plate, (h)& (i)* ***2e*** *in planar cell at 95°C under electric field 0V and 15V/ µm, 10Hz (j)* ***2i*** *at 109°C showing isotropic to nematic transition (Inset: fan-shaped texture); (k) & (l) optical micrographs of* ***2i*** *in planar cells at 0V and 20Vµm^{-1} ,10Hz at 104.5^{O}C.*

3.2 Electro-optical studies:

We have investigated the current responses in these mesogens applying a triangular wave voltage. Distinct current peaks are observed per half cycle of the applied voltage. In **1b** and **1c** two well-separated current humps are present in the SmA phase (**Figure 3(a)** and 3**(b)**). This indicates to the antiferroelectric nature of the smectic phase. The threshold voltage at which peaks appear prominently is 12Vµm^{-1} for **1b** (**Figure 3(a) inset**). **Figure 3(b)** shows evolution of the current peaks with temperature for **1c.** The two peaks A and B disappear completely as the isotropic phase is approached indicating pure polar origin of the peaks. Relatively broader peak B suggests two overlapped processes.

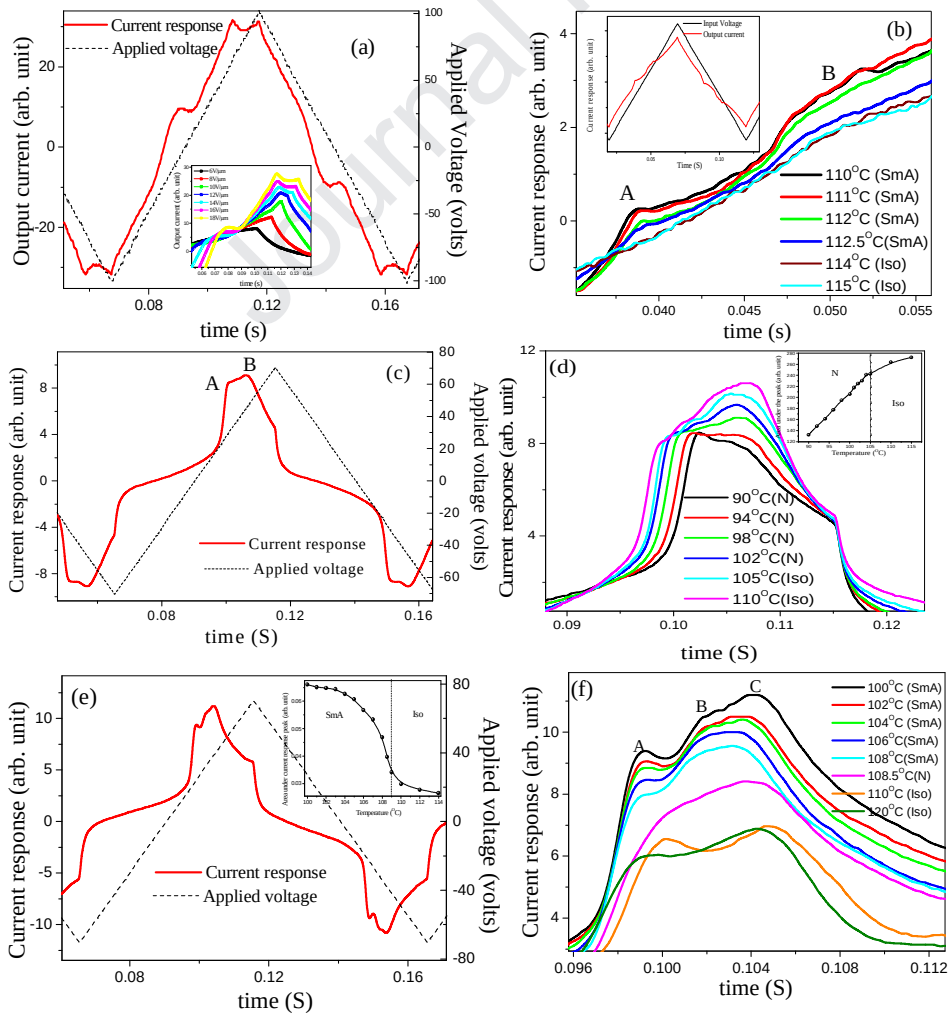

*Figure 3. (a) Current response curve of **1b** at110^{O}C applying triangular voltage 100V_{PP}, 10 Hz (Inset: voltage dependence of current response at frequency 10 Hz), (b) Current response curve of **1c** at different temperatures applying triangular voltage 90V_{PP}, 10Hz (Inset: variation of current response in a full cycle of applied triangular voltage at 110°C), (c) Current response curve of **2e** at 98°C applying triangular voltage 70V_{PP}, 10Hz, (d) Current response curve of **2e** at different temperatures applying triangular voltage 70V_{PP}, 10Hz (Inset: temperature dependence of area under the peak of current response), (e)Current response curve of **2i** at 100°C applying triangular voltage 70V_{PP}, 10Hz (Inset: temperature dependence of area under the peak of current response), (f) evolution of the three peaks in the current response curve with temperature for **2i** applying triangular voltage 70V_{PP}, 10 Hz.*

The compound **2e** exhibits two closely spaced current peaks on application of triangular electric field and their development over temperature is studied (**Figure 3(c)** and **3(d)**). Peak A is almost negligible in isotropic phase and becomes prominent with reduction of temperature. Since the molecular structure of these mesogens involve an OH group which is capable of proton conductivity and can easily complex ions to provide a current peak, the ionic contribution to the current response should also be considered. Since the peak at right (peak B) is growing with temperature and present in the isotropic phase, it may have partly ionic origin. Thus Peak A can be attributed to purely polar origin whereas peak B is a combination of polar and ionic contribution. Area under the peak is calculated for different temperatures and seems to increase continuously throughout the nematic phase and has high saturated value in the isotropic phase (**Figure 3(d) inset**).

The other compound **2i** shows similar current peaks in the SmA phase, however the broad overlapped peak in the right side now can be separated. Hence we have now three peaks A, B and C (**Figure 3(e)**). The peaks do not grow with temperature and suppresses appreciably in the isotropic phase (**Figure 3(f)**). Here it can be noticed that the short range nematic phase also shows polar switching and can be identified as cybotactic nematic phase. The area of the current peak gradually diminishes with increase of temperature suggesting typical orthogonal smectic nature of the phase.

3.3 Dielectric spectroscopy: The dielectric spectroscopy is a useful tool to study the molecular dynamics of liquid crystals. Dielectric investigations of the compounds **2e** and **2i** were carried out in planar aligned cells with thickness of 4 μm in the frequency range 10Hz to 13MHz, at

various temperatures. The frequency dependence of the complex dielectric permittivity in the specified conditions is described by the superposition of the Havriliak–Negami fit function and conductivity contribution. Characteristic dielectric parameters such as dielectric strength and relaxation frequency were extracted after incorporating the dielectric data into the following extended Havriliak–Negami function equation.

$$\varepsilon'' = \frac{\sigma_0}{\varepsilon_0} \times \frac{1}{\omega^s} + \sum_{k=1}^{N} \mathrm{Im}\left\{\frac{\Delta\varepsilon_k}{\left(1+(iw\tau_k)^{\alpha_k}\right)^{\beta_k}}\right\} \quad \text{.....(1)}$$

Where $\Delta\varepsilon_k$ is the dielectric strength and $\tau_k$is relaxation time of each individual process k involved in dielectric relaxation, ε_0 is the vacuum permittivity (8.854 pF/m) and σ_0 is the conduction parameter. The exponents α and β are empirical fit parameters, which describes a symmetric and non-symmetric broadening, respectively, of the relaxation peaks. The exponent s of the angular frequency determines the nonlinearity of the dc conductivity arising from charge accumulation at the interfacial layers. In the case of an Ohmic behaviour s=1.

Two compounds **2i** exhibiting SmA and a very narrow range nematic phase and **2e** exhibiting monotropic nematic phase were investigated by dielectric spectroscopy with a weak applied field (0.1 Vμm^{-1}) in the frequency range 10 Hz to 13MHz and at different temperatures in the SmA phase of **2i**. Dielectric investigations are carried out for the hockey-stick compound **2i** in SmA phase (30°C) in planar aligned cells with thickness 4 μm.

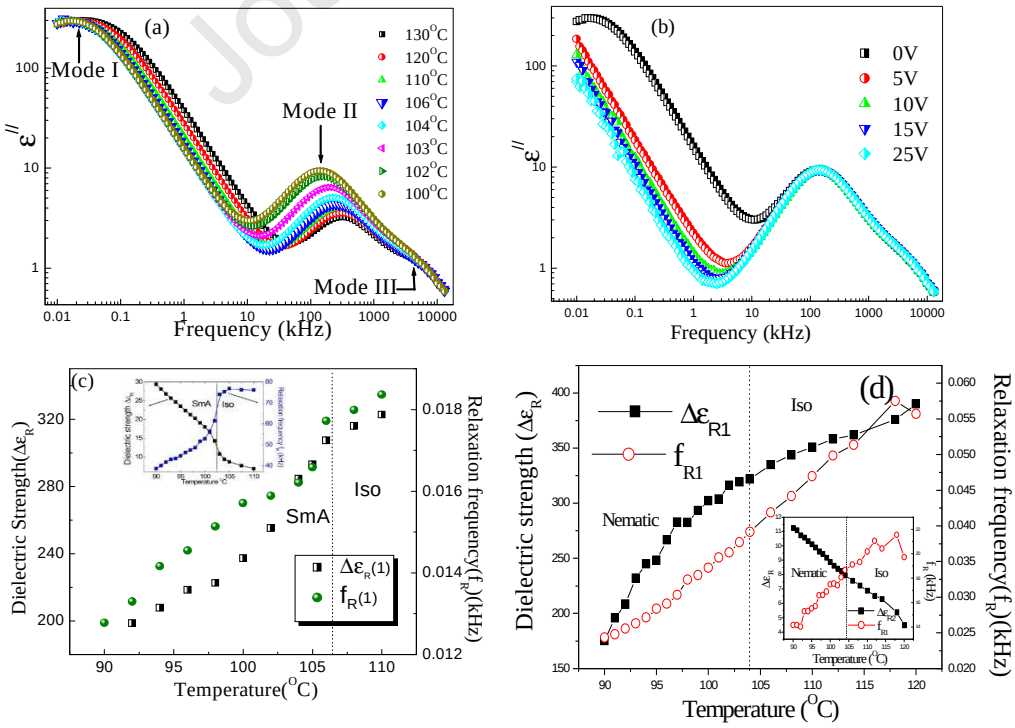

*Figure 4. Dielectric investigations of **2i:** (a) Dielectric spectra at different temperatures, (b) effect of bias voltage on relaxation peaks at 100°C, (c) temperature dependence of dielectric strength ($\Delta\varepsilon_R$) and relaxation frequency (f_R) of Mode I (Inset: variations of $\Delta\varepsilon_R$ and f_R with temperature for mode II); (d) temperature dependence of dielectric strength ($\Delta\varepsilon_R$) and relaxation frequency (f_R) of P1 for **2e** (Inset: variations of $\Delta\varepsilon_R$ and f_R with temperature for P2).*

The compound **2i** exhibited three relaxation modes in the smectic A phase and also in the fluid phase. Typical dielectric spectra variations at different temperatures are shown in **Figure 4(a)**. Due to narrow range of nematic phase the data was not recorded in nematic phase because of experimental limitation. The influence of bias voltage on the relaxation peaks is shown in **Figure 4(b)**. The low frequency mode (Mode I) ranging between 12 Hz and 20 Hz is a collective process as it gets suppressed totally under an applied bias voltage (**Figure 4(b)**). This peak can be ascribed to the formation of ferroelectric clusters even in isotropic phase. The dielectric strength ($\Delta\varepsilon_R$(I)) and relaxation frequency (f_R(I)) decreases upon cooling (**Figure 4(c)**).The large dielectric permittivity in low frequency region with low relaxation frequency indicates the presence of a strong positive dipolar correlation and dipole cooperative motions in the SmA phase. These characteristic features reflect the ferroelectric short range order in this phase.

The other mode at high frequency range defined as Mode II (kHz region) can be attributed to molecular processes as it is not suppressed by bias voltage. Mode II is due to rotation of the molecules around the short axis. $\Delta\varepsilon_R$(II) increases while f_R(II) decreases upon cooling (**Figure 3c inset**). The increase in relaxation frequency with an increase in temperature for both Mode I and II is due to reduction of viscosity of the material (**Figure 4(c)**). Similar relaxation modes could be found in the calamitic nematic LCs in GHz regime. Here the down shift of the relaxation frequencies of these modes can be because of high viscosity of the medium and its large molecular size. Mode III is assigned to ITO relaxation as it is independent of both bias voltage and temperature. Similar results are reported previously for few other bent-core materials exhibiting smectic A phase with random polarization ($SmAP_R$) inside the layers.
The compound **2e** exhibits two peaks; one (P1) at very low frequency (12-18 Hz) region and another (P2) at high frequency (40-80 kHz) rangeThe peaks have similar polar and molecular origin as its higher homologue. The variations of dielectric strength and relaxation frequency with temperature of these peaks are studied (**Figure 4(d)**).

3.4 XRD investigations: To get information on the conformation of the nematic phase of the compound **2e**, we carried out the XRD measurements. On cooling the sample from the isotropic phase down to ~ 1° above the isotropic - nematic phase transition, only a diffuse wide angle peak corresponding to the fluid-like ordering is revealed in the diffraction pattern. But as the temperature is decreased further and the sample enters to nematic phase, a distinct peak starts emerging in the small angle region (**Figure 5**), well above the nematic to crystal transition temperature ($T_{N\text{-}Cr}$~13°C). Hence this peak can be attributed to the formation of cybotactic clusters in the nematic phase and not due to start of crystallization. On further cooling in the nematic phase, the peak in the small angle region becomes gradually sharper (**Figure 5 inset**) with corresponding layer spacing d~3.24nm at 91°C. From DFT studies we have found the length (l) of the molecule to be 3.22nm. Thus the d to l ratio is ~1, which indicates that the clusters are of SmA type. This is clearly sharper than diffuse small angle peak of conventional nematics. Hence, this might indicate the cybotactic nature of the nematic phase (probably clusters with lamellar order).

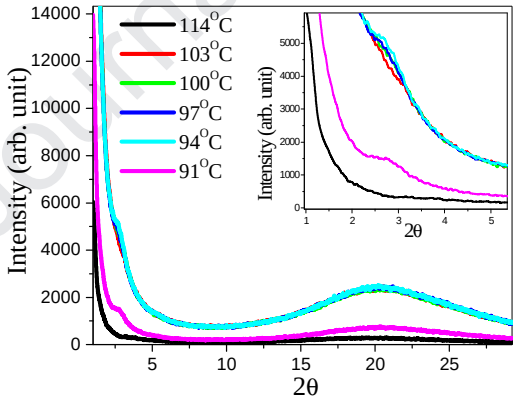

*Figure 5. X-ray diffraction studies of **2e**. Intensity profiles in the isotropic and nematic phases. Inset: Enlarged view of the small angle peak at 2θ~2.8°.*

4. Conclusion:

In conclusion we have designed, synthesized and characterized new achiral unsymmetrical four -ring hockey-stick compounds with a biphenyl moiety with polar substituents in the transverse and lateral directions of the molecule successfully. We further performed the measurements of

the induced polarization in two homologous series of hockey-stick liquid crystals, one exhibiting nematic as well as SmAP phase and the other exhibiting only SmAP in a cell of thicknesses of 4 μm with homogeneous alignment. The most interesting observation is the existence of polar switching in the entire nematic and isotropic phases of the material **2e** and the SmAP phase exhibited by **2i**, **1b** and **1c**. Dielectric investigation has complemented the electro-optically obtained results. X-ray analysis confirms the existence of cybotactic clusters in the nematic phase of **2e**. On the basis of these investigations it is clear that the hockey-stick molecules stick together to form clusters of cybotactic groups featuring short range SmA-like ordering in the nematic phase and even manifest themselves in isotropic phase because of polar interactions. We believe the present study would give significant insight to the development of ferroelectric fluids with overall polar order.

Acknowledgements: Author SG is grateful to the Department of Science and Technology, India for supporting this work under **INSPIRE Faculty Award** (IFA-13, PH-60) scheme.

References:

[1] T. Niori, T. Sekine, J. Watanabe, T. Furukawa, H. Takezoe, Distinct ferroelectric smectic liquid crystals consisting of banana shaped achiral molecules, J. Mater. Chem. 6 (1996) 1231-1233.

[2] R.A. Reddy, C. Tschierske, Bent-core liquid crystals: polar order, superstructural chirality and spontaneous desymmetrisation in soft matter systems, J. Mater. Chem. 16 (2006) 907-961.

[3] H. Takezoe, Y. Takanishi, Bent-Core Liquid Crystals: Their Mysterious and Attractive World J. Appl. Phys. 45 (2006) 597-625.

[4] W. Weissflog, H.N.S. Murthy, S. Diele, G. Pelzl, Relationships between molecular structure and physical properties in bent-core mesogens, Philos. Trans. R. Soc. A, 364 (2006) 2657-2679.

[5] R.A. Reddy, C. Zhu, R. Shao, E. Korblova, T. Gong, Y. Shen, E. Garcia, M.A. Glaser, J.E. Maclennan, D.M. Walba, N.A. Clark, Spontaneous Ferroelectric Order in a Bent-Core Smectic Liquid Crystal of Fluid Orthorhombic Layers, Science, 332 (2011) 72-77.

[6] Y. Shen, T. Gong, R.F. Shao, E. Korblova, J.E. Maclennan, D.M. Walba, N.A. Clark, Effective conductivity due to continuous polarization reorientation in fluid ferroelectrics, Phys, Rev. E. 84 (2011) 020701(R) (1-4).

[7] L.F. Guo, E. Gorecka, D. Pociecha, N. Vaupotic, M. Cepic, R.A. Reddy, K. Gornik, F. Araoka, N.A. Clark, D.M. Walba, K. Ishikawa, H. Takezoe, Ferroelectric behavior of

orthogonal smectic phase made of bent-core molecules, Phys. Rev. E. 84 (2011) 031706 (1-8).

[8] C. Zhu, R. Shao, R.A. Reddy, D. Chen, Y. Shen, T. Gong, M.A. Glaser, E. Korblova, P. Rudquist, J.E. Maclennan, D.M. Walba, N.A. Clark, Topological Ferroelectric Bistability in a Polarization-Modulated Orthogonal Smectic Liquid Crystal, J. Am. Chem. Soc. 134 (2012) 9681-9687.

[9] A. Eremin, S. Diele, G. Pelzl, H. Nádasi, W. Weissfiog, J. Salfetnikova, H. Kresse, Experimental evidence for an achiral orthogonal biaxial smectic phase without in-plane order exhibiting antiferroelectric switching behaviour, Phys. Rev. 64 (2001) 051707 (1-6).

[10] M.W. Schroder, S. Diele, N. Pancenko, W. Weissflog, G. Pelzl, Evidence for a polar biaxial SmA phase (C_{PA}) in the sequence SmA–C_{PA}–B_2, J. Mater. Chem. 12 (2002) 1331-1334.

[11] L.E. Hough, M. Spannuth, M. Nakata, D.A. Coleman, C.D. Jones, G. Dantlgraber, C. Tschierske, J. Watanabe, E. Körblova, D.M. Walba, J.E. Maclennan, Chiral isotropic liquids from achiral molecules. Science. 325 (2009) 452-456.

[12] C. Keith, M. Prehm, Y.P. Panarin, J.K. Vij, C. Tschierske, Development of polar order in liquid crystalline phases of a banana compound with a unique sequence of three orthogonal phases, Chem. Commun. 46 (2010) 3702-3704.

[13] Y.P. Panarin, M. Nagaraj, J.K. Vij, C. Keith, C. Tschierske, Field-induced transformations in the biaxial order of non-tilted phases in a bent-core smectic liquid crystal, Euro-PhysLett. 92 (2010) 26002 (1-6).

[14] M. Nagaraj, Y.P. Panarin, J.K. Vij, C. Keith, C. Tschierske, Liquid crystal display modes in a nontilted bent-core biaxial smectic liquid crystal, Appl. Phys Lett. 97 (2010) 213505 (1-3).

[15] L. Kovalenko, M.W. Schroder, R.A. Reddy, S. Diele, G. Pelzl, W. Weissflog, Unusual mesomorphic behaviour of new bent-core mesogens derived from 4-cyanoresorcinol, Liq. Cryst. 32 (2005) 857-865.

[16] R.A. Reddy, B.K. Sadashiva, Direct transition from a nematic phase to a polar biaxial smectic A phase in a homologous series of unsymmetrically substituted bent-core compounds, J. Mater. Chem. 14 (2004) 310-319.

[17] B. Glettner, S. Hein, R.A. Reddy, U. Baumeister, C. Tschierske, Cyclic ureas as novel building blocks for bent-core liquid crystals, Chem. Commun. 25 (2007) 2596-2598.

[18] L. Guo , S. Dhara , B.K. Sadashiva , S. Rasdhika , R. Prathiba, Y. Shimbo, F. Araoka, K. Ishikawa, H. Takezoe, Polar switching in the smectic-AdPA phase composed of asymmetric bent-core molecules, Phys. Rev. E, 81 (2010) 011703 (1-6).

[19] D. Pociecha, M. Cepic, E. Gorecka, J. Mieczkowski, Ferroelectric Mesophase with Randomized Interlayer Structure, Phys. Rev. Lett. 91 (2003) 185501 (1-4).

[20] Y. Shimbo, E. Gorecka, D. Pociecha, F. Araoka, M. Goto,Y. Takanishi, K. Ishikawa, J. Mieczkowski, K. Gomola, H. Takezoe, Electric-Field-Induced Polar Biaxial Order in a Nontilted Smectic Phase of an Asymmetric Bent-Core Liquid Crystal Phys. Rev. Lett. 97 (2006) 113901 (1-4).

[21] K. Gomola, L. Guo, S. Dhara, Y. Shimbo, E. Gorecka, D. Pociecha, J. Mieczkowski, H. Takezoe, Syntheses and characterization of novel asymmetric bent-core mesogens exhibiting polar smectic phases, J. Mater. Chem, 19 (2009) 4240-4247.

[22] K. Gomola, L. Guo, E. Gorecka, D. Pociecha, J. Mieczkowski, K. Ishikawa, H. Takezoe, First symmetrical banana compounds exhibiting SmAPR mesophase and unique transition between two orthogonal polar phases, Chem. Comm. 43 (2009) 6592-6594.

[23] Y. Shimbo, Y. Takanishi, K. Ishikawa, E. Gorecka, D. Pociecha, J. Mieczkowski, K. Gomola, H. Takezoe, Ideal Liquid Crystal Display Mode Using Achiral Banana-Shaped Liquid Crystals, Jpn. J. Appl. Phys. 45 (2006) L282.

[24] M. Gupta, S. Datta, S. Radhika, B.K. Sadashiva, A. Roy, Randomly polarised smectic A phase exhibited by bent-core molecules: experimental and theoretical studies, Soft Matter, 7 (2011) 4735-4741.

[25] C. Tschierske, D.J. Photinos, Biaxial nematic phases, J. Mater. Chem. 20 (2010) 4263-4294.

[26] R. Berardi, M. Ricci, C. Zannoni, Ferroelectric Nematic and Smectic Liquid Crystals from Tapered Molecules, ChemPhysChem, 2 (2001) 443-447.

[27] (a) J.-H. Lee, T.-K. Lim, W.-T. Kim, and J.-I. Jin, J. Appl. Phys. 101 (2007) 034105; (b) R. Stannarius, J. Appl. Phys. 104 (2008) 036104.

[28] O. Francescangeli, V. Stanic, S.I. Torgova, A. Strigazzi, N. Scaramuzza, C. Ferrero, I.P. Dolbnya, T.M. Weiss, R. Berardi, L. Muccioli, S. Orlandi, C. Zannoni, Ferroelectric Response and Induced Biaxiality in the Nematic Phase of Bent-Core Mesogens, Adv. Funct. Mater. 19 (2009) 2592-2600.

[29] G. Shanker, M. Nagaraj, A. Kocot, J.K. Vij, M. Prehm, C. Tschierske, Nematic Phases in 1,2,4-Oxadiazole-Based Bent-Core Liquid Crystals: Is There a Ferroelectric Switching? Adv. Funct. Mater. 22 (2012) 1671-1683.

[30] J. Harden, B. Mbanga, N. Eber, K. Fodor-Csorba, S. Sprunt, J.T. Gleeson, A. Jakli, Giant Flexoelectricity of Bent-Core Nematic Liquid Crystals, Phys. Rev. Lett. 97 (2006) 157802 (1-4).

[31] R.J. Mandle, E.J. Davis, C.T. Archbold, C.C.A. Voll, J.L. Andrews, S.J. Cowling, John W. Goodby, Apolar Bimesogens and the Incidence of the Twist–Bend Nematic Phase, Chemistry-A European Journal. 21 (2015) 8158-8167.

[32] S.M. Jansze, A. Martínez-Felipe, J.M.D. Storey, A.T.M. Marcelis, C.T. Imrie, A Twist-Bend Nematic Phase Driven by Hydrogen Bonding, Angew Chem Int Ed. 54 (2015) 643-646.

[33] E. Gorecka, M. Salamonczyk, A. Zep, D. Pociecha, C. Welch, Z. Ahmed, G.H. Mehl, Do the short helices exist in the nematic TB phase? Liq. Cryst. 42 (2015) 1-7.

[34] A. Jakli, Liquid crystals of the twenty-first century – nematic phase of bent-core molecules, *Liquid Crystals Reviews*, 1 (2013) 65–82.

[35] S. Ghosh, N. Begum, S. Turlapati, S.K.Roy, A.K. Das, N.V.S. Rao, Ferroelectric-like switching in the nematic phase of four-ring bent-core liquid crystals, J. Mater. Chem. C. 2 (2014) 425-431.

[36] S. Turlapati, R. K. Khan, S. Ghosh, P. Tadapatri, R. Pratibha and N. V. S. Rao, Existence of polar switching in the nematic and orthogonal smectic phases in novel four-ring bent-core compounds, J. Appl. Phys. 120 (2016) 174101.

[37] R. K. Khan, S. Turlapati, N. Begum, G. Mohiuddin, N. V. S. Rao and S. Ghosh, Impact of terminal polar substitution on elastic, electro-optic and dielectric properties of four-ring bent-core nematic liquid crystals RSC Adv. 8(2018) 11509.

[38] P. Sathyanarayana, S. Radhika, B. K. Sadashiva and Surajit Dhara, Structure–property correlation of a hockey stick-shaped compound exhibiting N-SmA-SmCa phase transitions, Soft Matter, 2012, 8, 2322-2327.

[39] D. Chen, H. Wang, M. Li, M. A. Glaser, J. E. Maclennan and N. A. Clark, Chiral random grain boundary phase of achiral hockey-stick liquid crystals, Soft Matter, 2014,10, 9105-9109.

[40] A. Chakraborty, M. Kumar Das, Banani Das, U. Baumeister and W. Weissflog, Optical, dielectric and visco-elastic properties of a few hockey stick-shaped liquid crystals with a lateral methyl group **,** J. Mater. Chem. C, 2013,1, 7418-7429.

[41] M. Alaasar, S. Poppe, C. Kerzig, C. Klopp, A. Eremin and C. Tschierske, Cluster phases of 4-cyanoresorcinol derived hockey-stick liquid crystals, J. Mater. Chem. C, 2017,5, 8454-8468.

Highlights:

- Investigations on novel short-core hockey-stick molecules are reported.
- The compounds exhibit nematic and orthogonal smectic mesomorphism.
- Cybotactic clusters in the nematic phase are confirmed by XRD.
- Polar orthogonal smectic phases with antiferroelectric type switching are observed.